Theoretical description of hadroproduction and production on nuclear targets of φ-mesons at very high energies

Carlos Merino

University of Santiago de Compostela

Galiza-Spain

in collaboration with

G.H. Arakelyan and Yu.M. Shabelski

carlos.merino@usc.es

I. Aim:

We consider the experimental data on φ-meson production in hadron-nucleon, pA, and AA collisions, for a wide energy region going up to the LHC range.

We compare with the results of the corresponding calculations obtained in the frame of the Quark-Gluon String Model (QGSM).

Phys. Rev. D90, 114019 (2014), Phys. At. Nucl. 80, 1197 (2017), and references therein.

II. Meson production in the Quark-Gluon String Model: inclusive spectra in pp, pA, and AA collisions

The QGSM is based on Dual Topological Unitarization, Regge phenomenology, and nonperturbative features of QCD.

The QGSM successfully describes multiparticle production in hadron-hadron and hadron-nucleus collisions.

High energy interactions proceed via the exchange of one or several Pomerons, and elastic and inelastic processes result from cutting between or through Pomerons.

In the case of multipomeron exchange, the distributions of valence quarks and diquarks are softened due to the appearance of a sea quark contribution.

For a nucleon target, the inclusive rapidity, y, or Feynman-x, x_F , spectrum of a secondary hadron h has the form

$$\frac{dn}{dy} = \frac{x_E}{\sigma_{inel}} \cdot \frac{d\sigma}{dy} = \sum_{n=1}^{\infty} \omega_n \cdot \Phi_n^h(x)$$

where the functions $\Phi_n^h(x)$ determine the contribution of diagrams with n cut Pomerons.

For pp collisions:

$$\phi_n^h(x) = f_{qq}^h(x_+,n)\cdot f_q^h(x_-,n) + f_q^h(x_+,n)\cdot f_{qq}^h(x_-,n) + 2(n-1) f_s^h(x_+,n)\cdot f_s^h(x_-,n) \ ,$$

$$x_\pm = \frac{1}{2}\left[\sqrt{4m_T^2/s + x^2} \pm x\right] \ ,$$

where f_{qq}, f_q, and f_s are the contributions of diquarks, valence quarks, and sea quarks, respectively.

The inclusive spectrum of a secondary hadron **h** is determined by the **convolution** of the diquark, valence quark, and sea quark distributions, **u(x, n)**, in the incident particles, with the fragmentation functions, $G^h(z)$, of quarks and diquarks into the secondary hadron **h**.

$$f_q^h(x_+, n) = \int_{x_+}^1 u_q(x_1, n) \cdot G_q^h(x_+/x_1) dx_1 \quad .$$

Both the distributions and the fragmentation functions are constructed using the Reggeon counting rules.

The values of the Pomeron parameters were fixed by performing a Regge fit to the experimental data on hadron-nucleon scattering up to the collider energies.

The cross sections of all inelastic processes corresponding to diagrams where $n \geq 1$ Pomerons are cut, can be calculated by using the AGK rules.

The distribution functions of quarks and diquarks in a colliding proton, for arbitrary n, are:

$$u_{uu}(x,n) = C_{uu}x^{\alpha_R-2\alpha_B+1}(1-x)^{-\alpha_R+\frac{4}{3}(n-1)},$$

$$u_{ud}(x,n) = C_{ud}x^{\alpha_R-2\alpha_B}(1-x)^{-\alpha_R+n-1},$$

$$u_{u}(x,n) = C_{u}x^{-\alpha_R}(1-x)^{\alpha_R-2\alpha_B+n-1},$$

$$u_{d}(x,n) = C_{d}x^{-\alpha_R}(1-x)^{\alpha_R-2\alpha_B+1+\frac{4}{3}(n-1)},$$

$$u_{s}(x,n) = C_{d}x^{-\alpha_R}(1-x)^{\alpha_R-2\alpha_B+n-1}.$$

The distribution functions of quarks and diquarks in a colliding π^-, for arbitrary n, are:

$$u_d(x,n) = u_{\bar{u}}(x,n) = C_d x^{-\alpha_R}(1-x)^{-\alpha_R+n-1},$$

$$u_u(x,n) = u_{\bar{d}}(x,n) = C_u x^{-\alpha_R}(1-x)^{-\alpha_R+n-1}\left[1-\delta\sqrt{1-x}\right],$$

$$n > 1,$$

$$u_{\bar{s}}(x,n) = C_{\bar{s}} x^{-\alpha_R}(1-x)^{n-1}, \qquad n > 1$$

The quark and diquark fragmentation functions into φ-mesons have the form:

$$G_u^{\varphi} = G_d^{\varphi} = G_{\bar{u}}^{\varphi} = G_{\bar{d}}^{\varphi} = a_{\varphi} \cdot (1-z)^{\lambda - \alpha_R - 2\alpha_{\varphi} + 2},$$

$$G_s^{\varphi} = G_{\bar{s}}^{\varphi} = a_{\varphi} \cdot (1-z)^{\lambda - \alpha_{\varphi}}.$$

$$G_{uu}^{\varphi} = G_{ud}^{\varphi} = a_{\varphi} \cdot (1-z)^{\lambda + \alpha_R - 2(\alpha_R + \alpha_{\varphi})}$$

where the parameter λ takes the value $\lambda = 0.5$, and $\alpha_R = 0.5$, and $\alpha_{\varphi}=0$. are the intercepts of the ρ and φ Regge trajectories, respectively.

The parameter a_φ represents the φ density in the central region of one Pomeron.

The value of a_φ is universal, since it neither depends on the energy, nor on the beam of the collision.

This value has been fixed, by simultaneously describing in a reasonable way most of the experimental data on φ production from pion and proton beams, to be $a_\varphi = 0.11$.

In the case of interaction with a nuclear target, the Gribov-Glauber theory is used (superposition of interactions with different numbers of target nucleons).

The quark and diquark distributions and fragmentation functions are identical to those in the case of p-nucleon interactions.

We also take the same values of the Pomeron parameters used for the description of pp collisions.

III. Description of the experimental data on hadroproduction of φ-mesons on a proton target:

We compare the results of the QGSM calculations with the experimental data on φ inclusive cross sections in πp and pp collisions at different energies up to the LHC range.

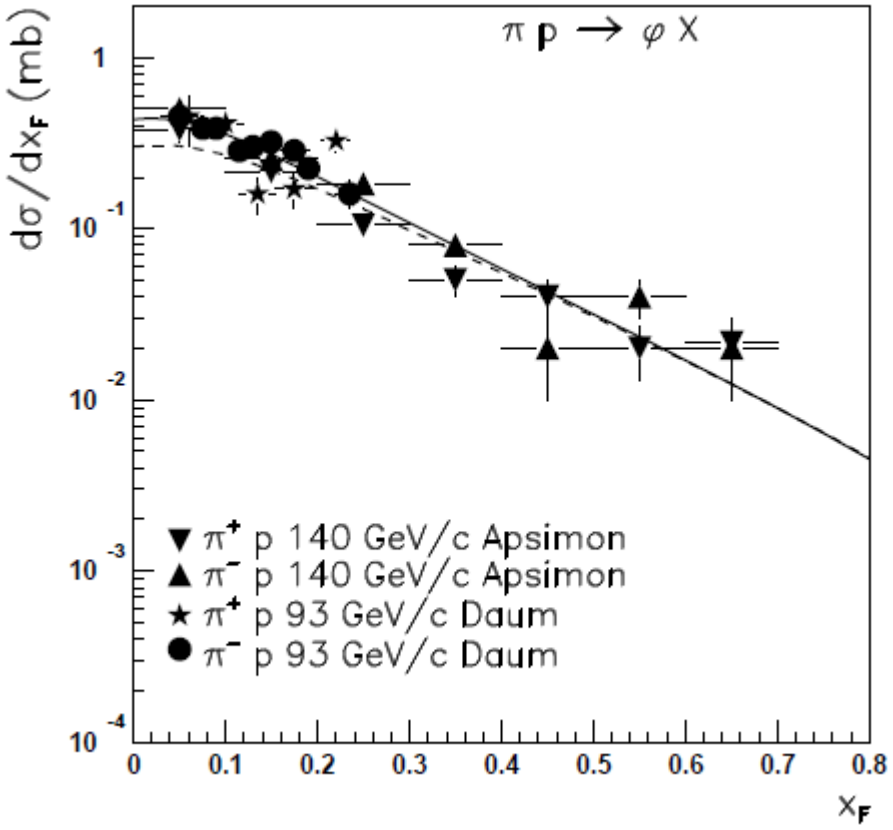

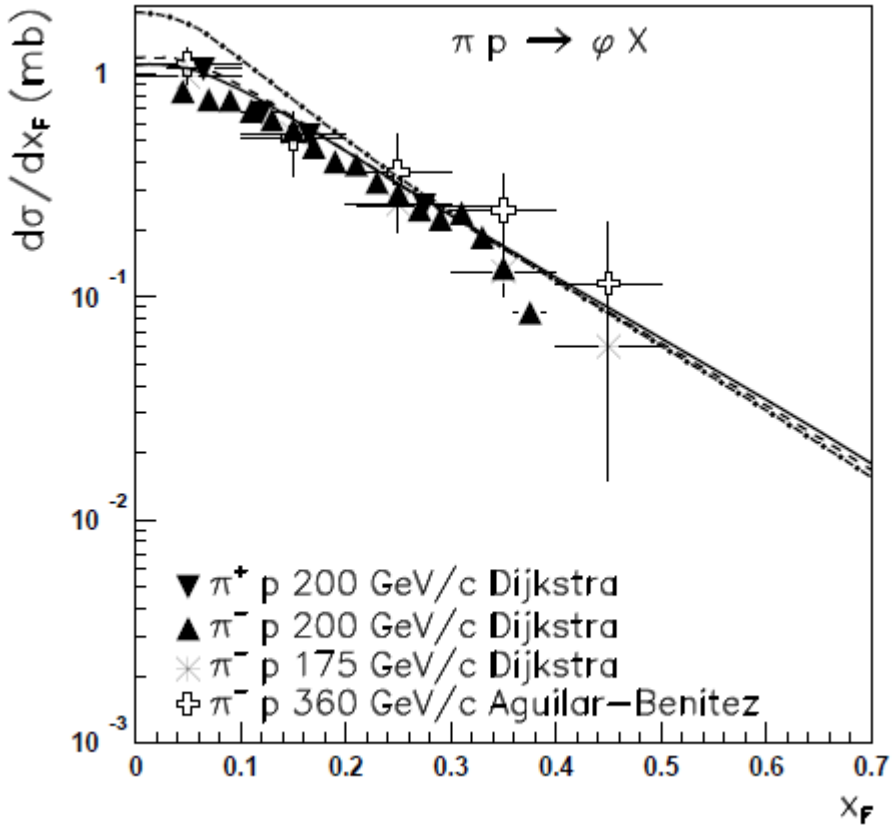

Experimental data on x_F-spectra of φ-mesons in $\pi^{\pm}$p collisions at different energies, compared to the corresponding QGSM results.

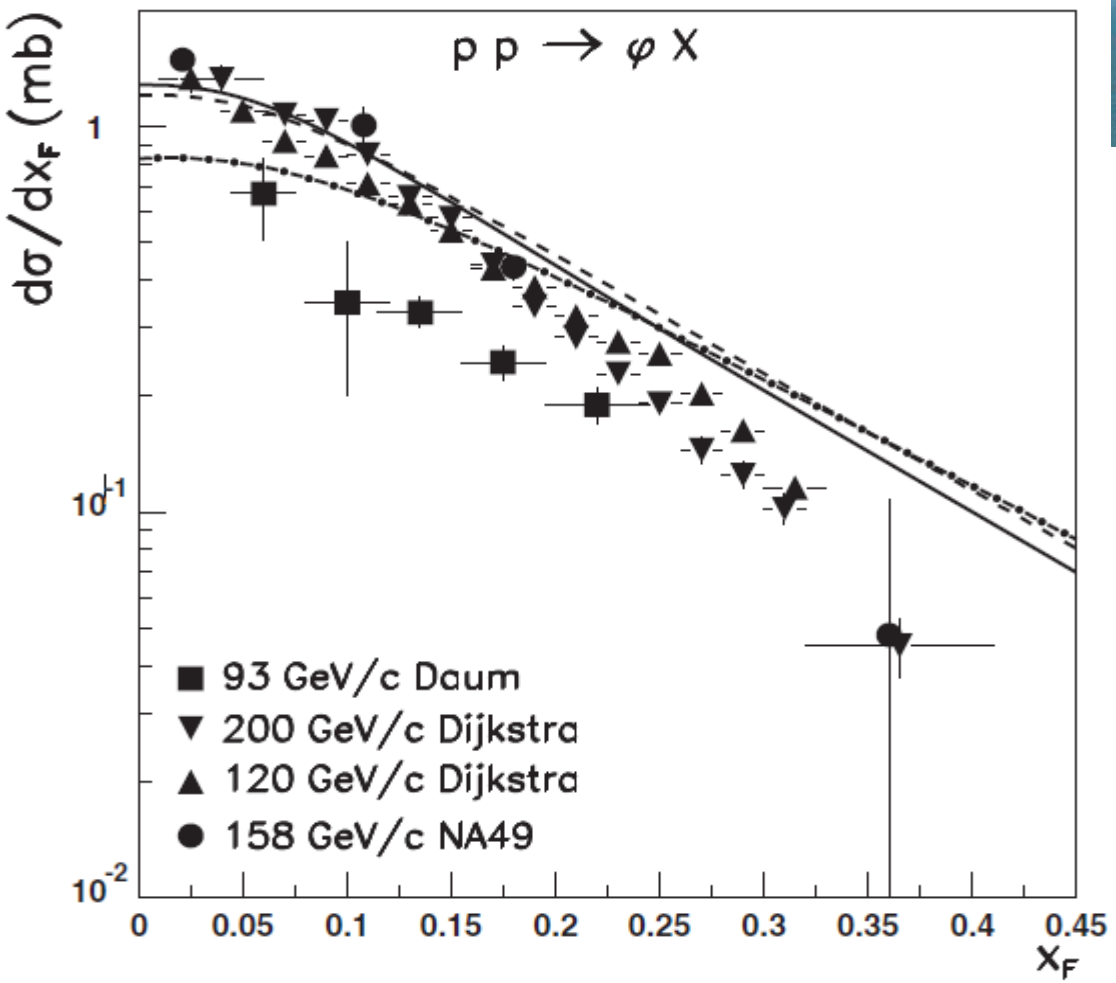

Experimental data on x_F-spectra of φ-mesons in pp collisions at 93, 120, 158, and 200 GeV/c, compared to the corresponding QGSM results at 93, 158, and 200 GeV/c.

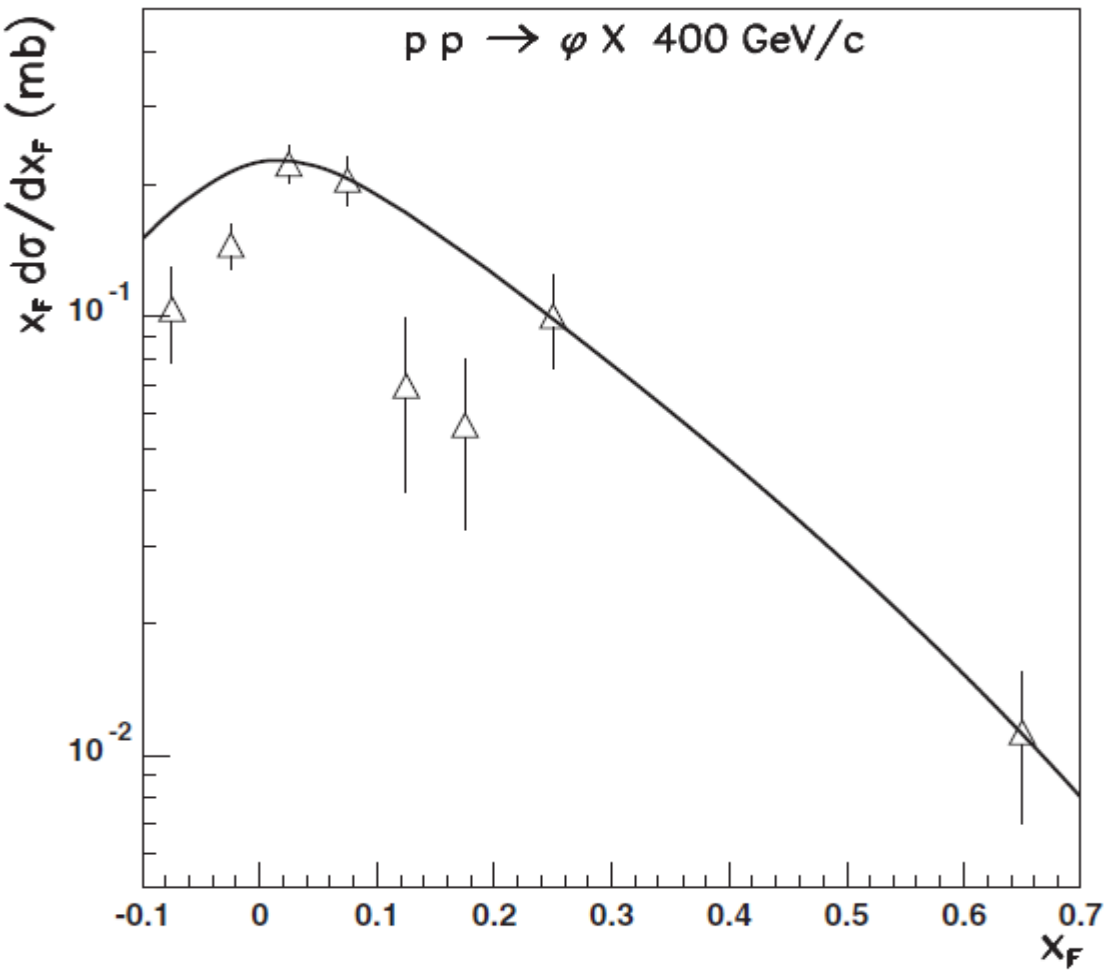

Experimental data on x_F-spectra of φ-mesons in pp collisions at 400 GeV/c (LEBC-EHS Collaboration), compared to the corresponding QGSM results.

K^+

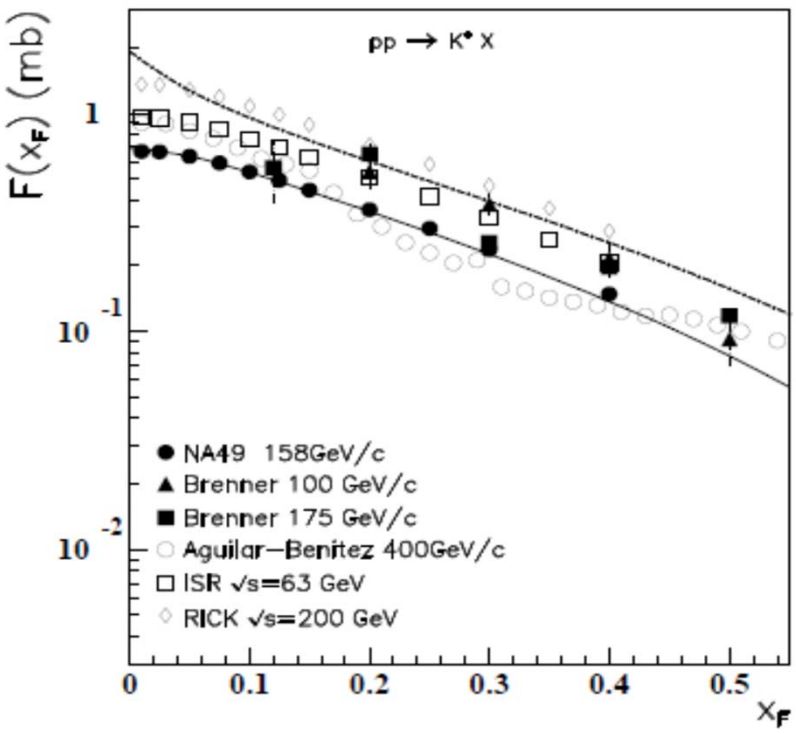

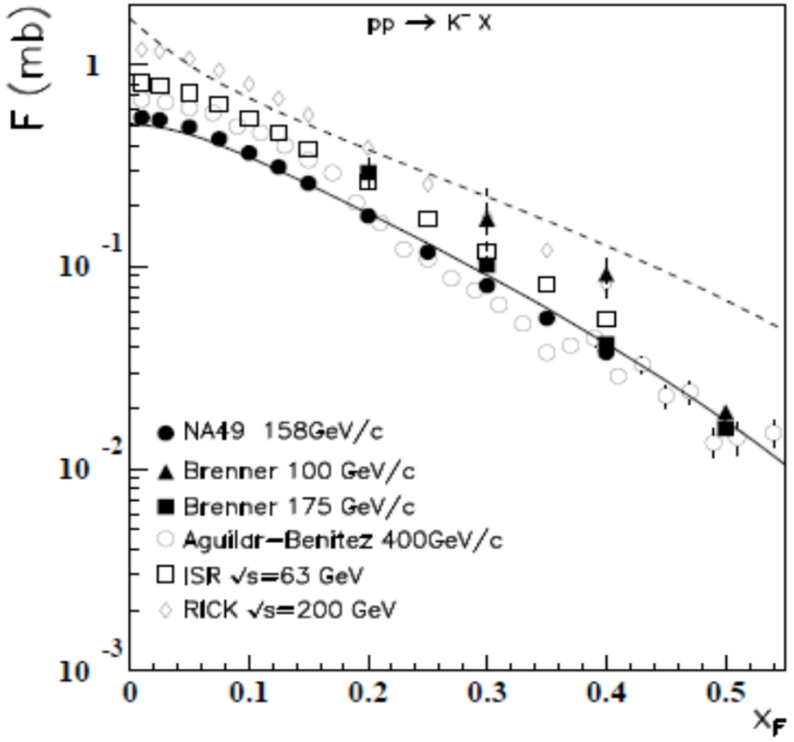

Experimental data on the invariant cross section of K^+ and K^- in pp collisions at different energies, compared to the corresponding QGSM results.

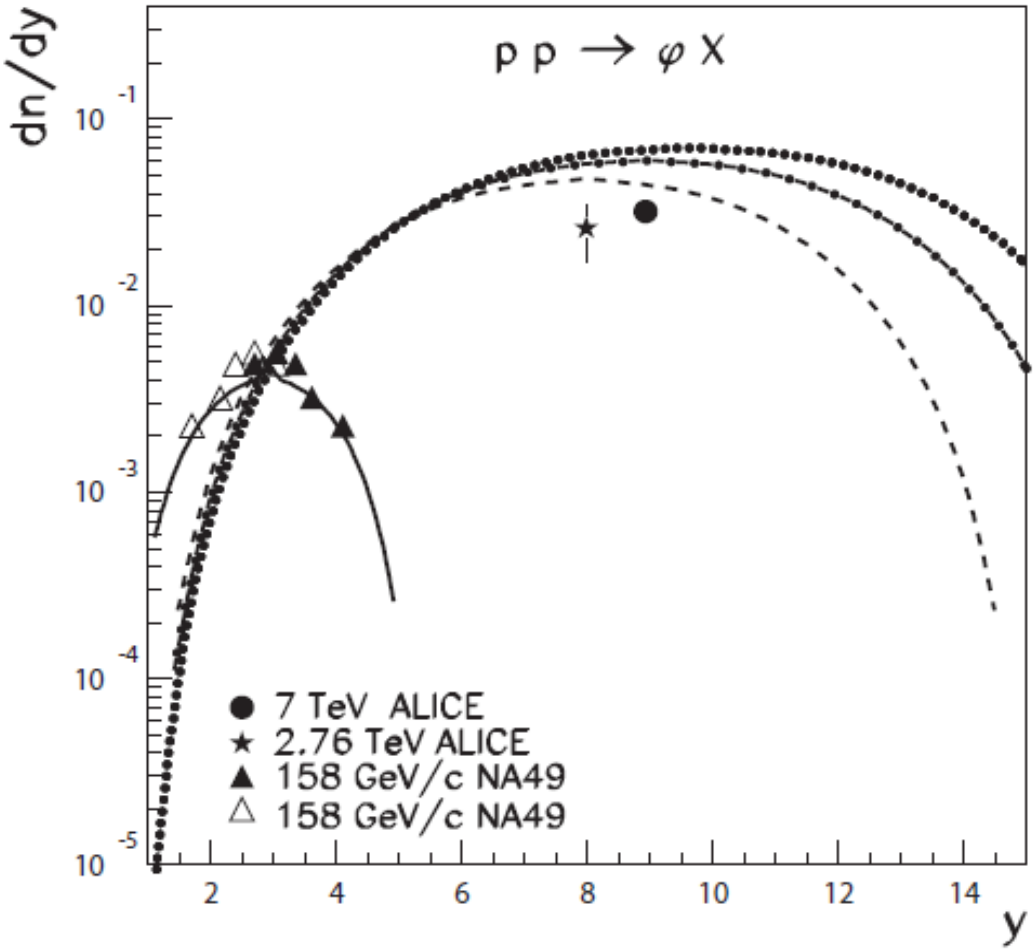

Experimental data on y-spectra, dn/dy, of φ-mesons in pp collisions at 158 GeV/c (LEBC-EHS Collaboration), compared to the corresponding QGSM results.

In this figure, the QGSM y-spectra, dn/dy, of φ-mesons in pp collisions for 2.76 TeV (dashed) and 7 TeV (dashed-dotted) are also presented, and compared to the corresponding experimental points at $|y| \leq 0.5$ (ALICE Collaboration).

The dotted curve is the QGSM prediction for 14 TeV.

In general, the QGSM description of the experimental data in the considered energy region, shown in previous figures, is consistent.

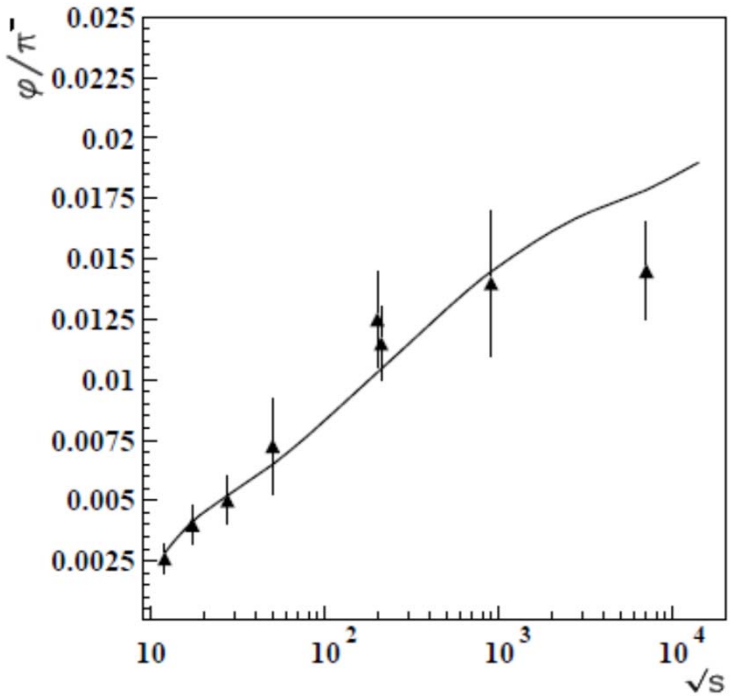

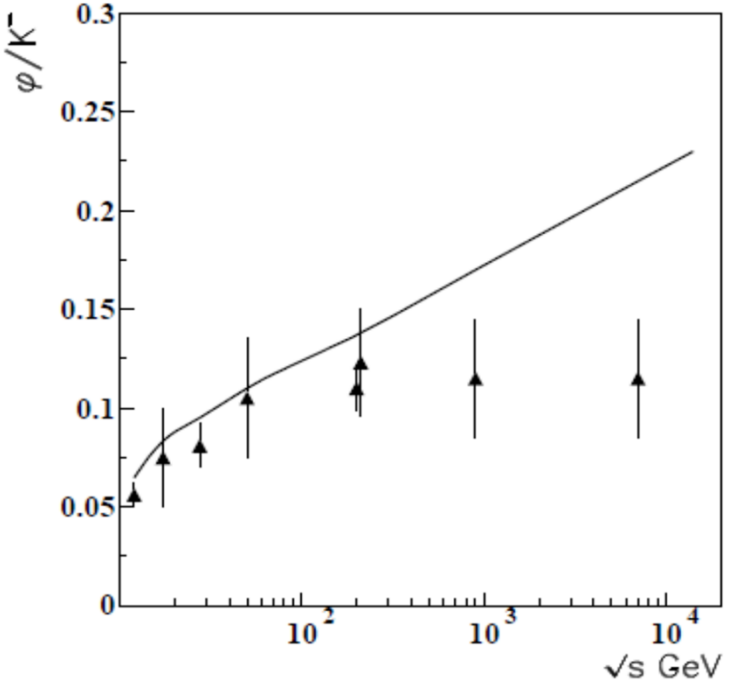

Experimental data on the $\sqrt{s}$ dependence of φ/π^- and φ/K^- cross section ratios in pp collisions, compared to the corresponding QGSM results.

IV. Production of φ-mesons on nuclear targets up to the RHIC energies

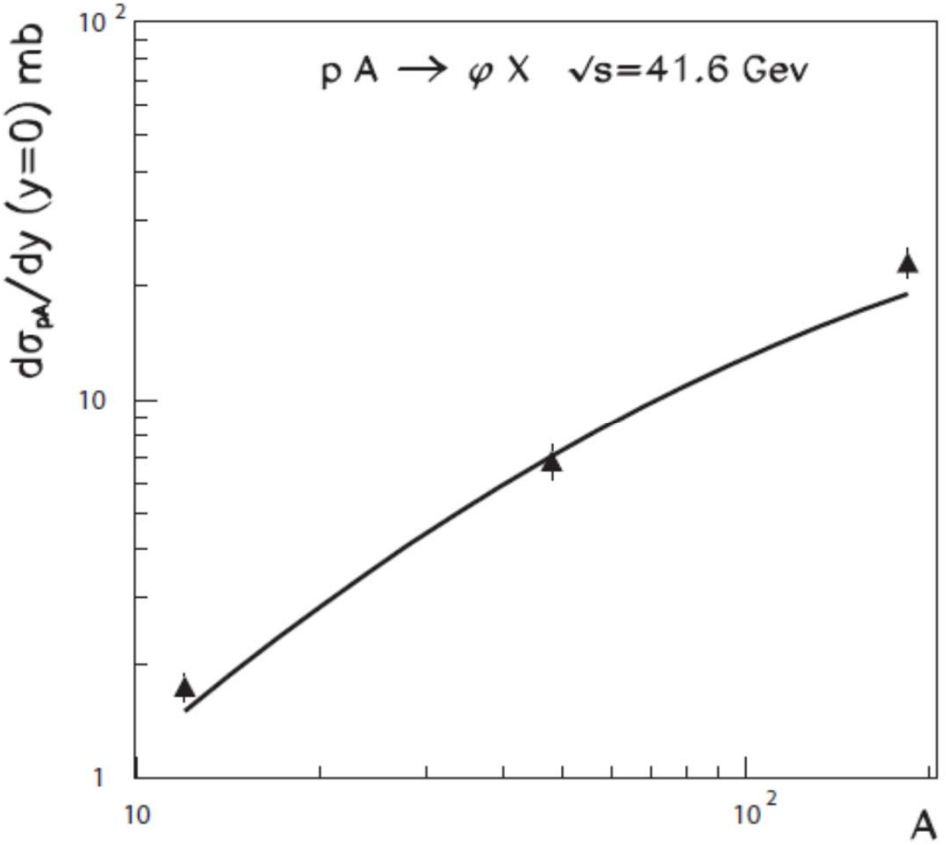

Experimental data on the A dependence of the cross sections for φ-meson production, dσ/dy, at midrapidity, in pA collisions at the energy $\sqrt{s}$ =41.6 GeV, compared to the results of the corresponding QGSM calculations.

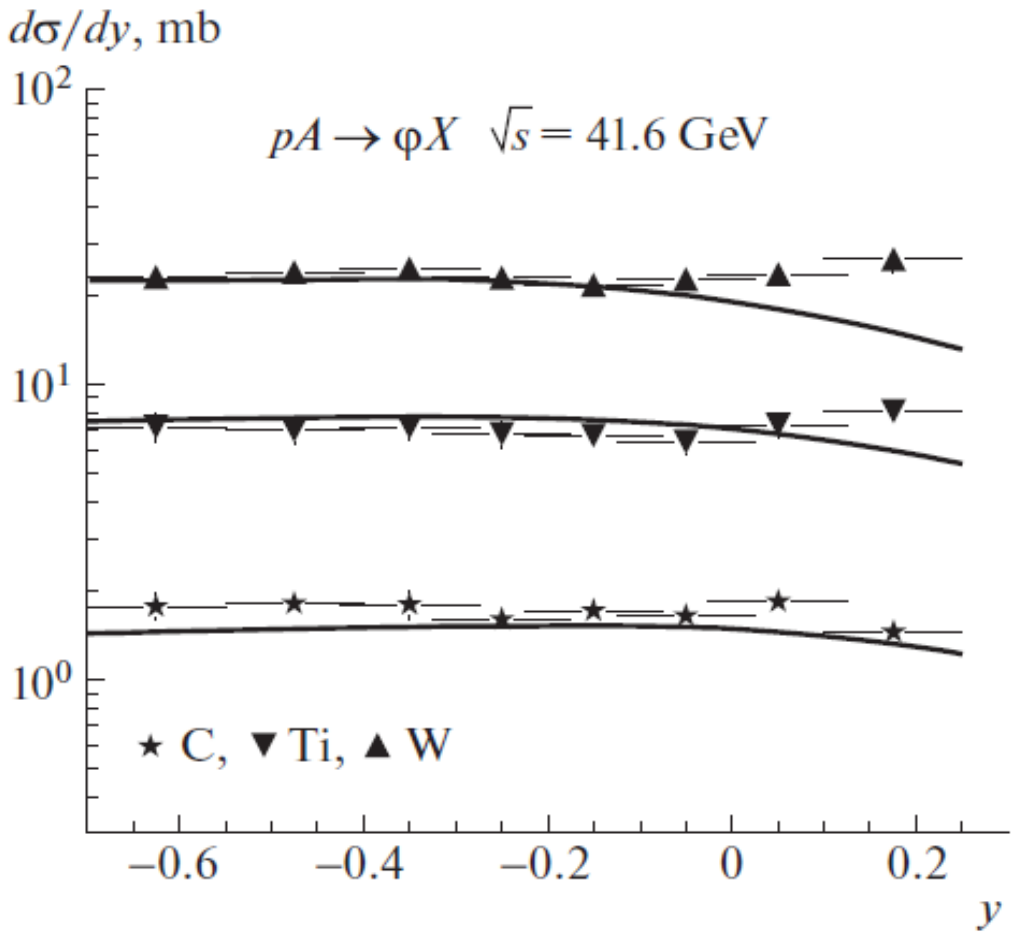

Experimental data on the y dependence of the cross sections for φ-meson production, dσ/dy, in pA collisions, where A=C,Ti, and W, at the energy $\sqrt{s}$ =41.6 GeV, compared to the results of the corresponding QGSM calculations.

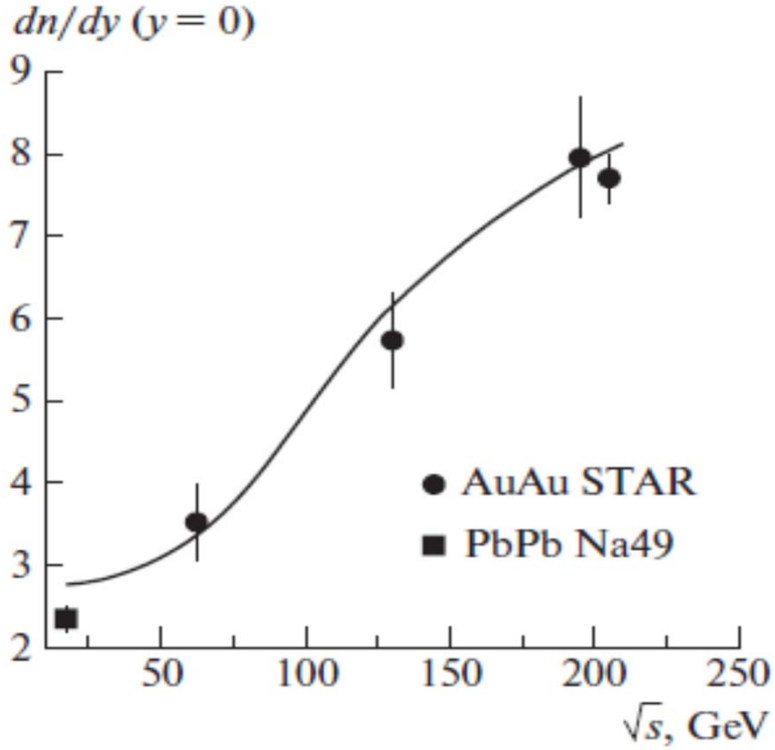

Experimental data on the $\sqrt{s}$ dependence of the inclusive density for φ-meson production, dn/dy, in the midrapidity region, in Au-Au and Pb-Pb collisions, compared to the results of the corresponding QGSM calculations.

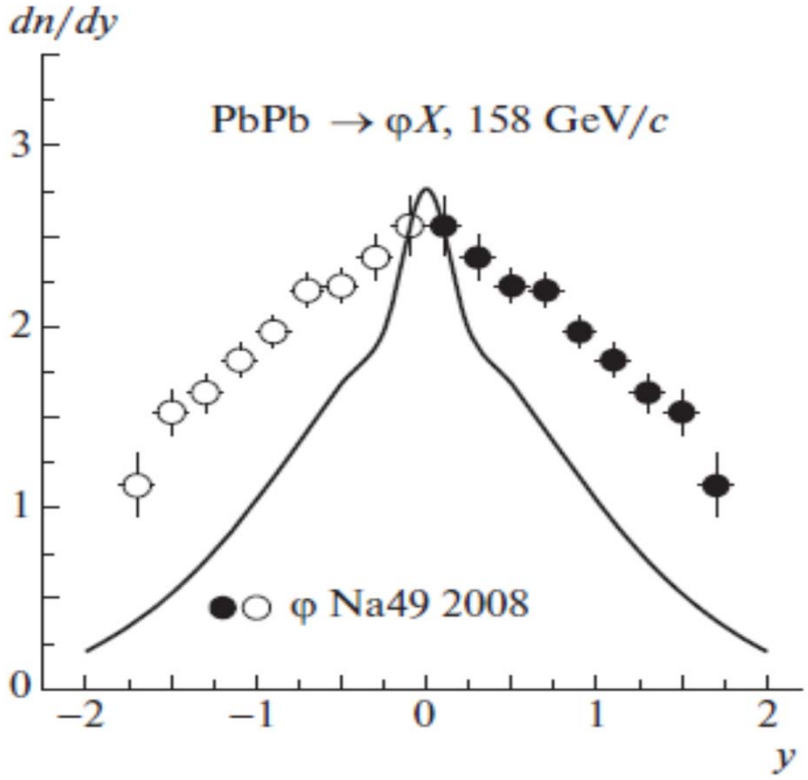

Experimental data on the y dependence of the inclusive density for φ-meson production, dn/dy, in Pb-Pb collisions at 158 GeV/c, compared to the results of the corresponding QGSM calculations.

In the case of φ-meson production, the inelastic-screening effects are negligible in the energy region up to RHIC, but they will be significant at LHC.

V. Production of φ-mesons in pPb and PbPb collisions at LHC energies

Saturation effects can be explained by corrections for inelastic shadowing connected to the multipomeron interactions (more and more important as the initial energy grows).

In the case of interactions with nuclei, the mean number of Pomerons is large, and their interactions become significant at LHC energies.

The percolation approach can be used to account for the inelastic shadowing in QGSM, by considering the maximal number of cut pomerons in the midrapidity region emitted by one nucleon (fitted to experimental data).

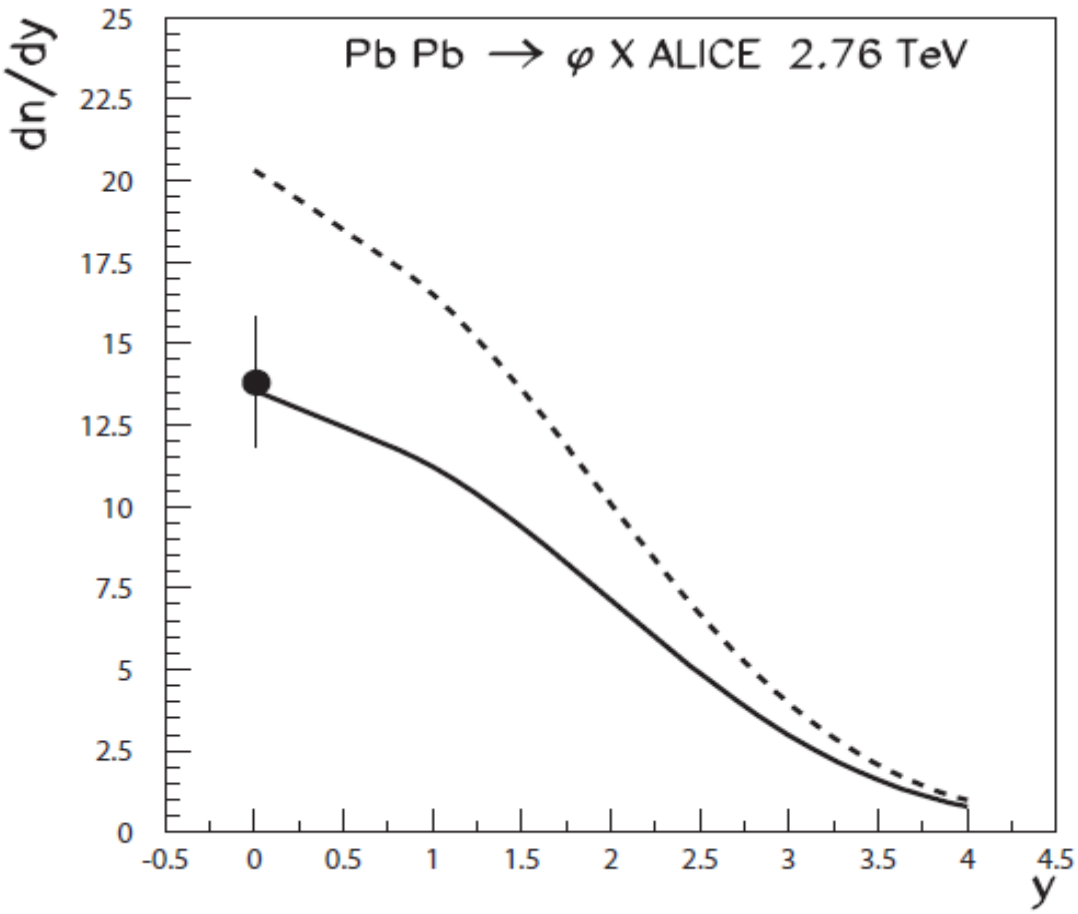

QGSM prediction for the rapidity dependence of the density for φ-meson production, dn/dy, in central Pb-Pb collisions at $\sqrt{s} = 2.76\,TeV$, with (full) and without (dashed curve) inelastic shadowing, compared to the ALICE experimental point.

VI. Conclusions (1)

The Quark-Gluon String Model provides a reasonable description of φ-production for the interaction of different hadron beams with a nucleon target, in a wide energy region going to the LHC range.

Up to RHIC energies, the QGSM also provides a reasonable description of φ-production for the interaction of p and nuclei with nuclear targets, without any additional parameter with respect to the case of pp collisions, and without including inelastic-shadowing effects.

VI. Conclusions (2)

The inelastic-shadowing effects in φ-production are markedly weaker than for production of $\pi^{\pm}$, $K^{\pm}$, p, and $\overline{p}$, and they become observable in collisions on a nuclear target, only at higher energies of $\sqrt{s}$ ≥ 1 TeV.

This behaviour may be due to a sizeable s quark mass.

VI. Conclusions (3)

The φ-meson production in pA and AA collisions at LHC energies, with accounting for inelastic-shadowing effects, can be calculated in QGSM by using the percolation approach.

In Pb-Pb collisions at $\sqrt{s}$ = 2.76 TeV, the inelastic-shadowing effect reduces the value of dn/dy (|y|≤0.5) for φ-meson production by a factor of about 1.5.